Geophysical Research Letters

RESEARCH LETTER
10.1029/2025GL118806

# Moisture Sources of Precipitation Using Convection-Permitting Simulations: A Study Over South America

**Erick Claros**[1], **Francina Dominguez**[2], **and Changhai Liu**[3]

[1]Department of Civil and Environmental Engineering, University of Illinois Urbana-Champaign, Urbana, IL, USA, [2]Department of Climate, Meteorology and Atmospheric Sciences, University of Illinois Urbana-Champaign, Urbana, IL, USA, [3]National Center for Atmospheric Research, Boulder, CO, USA

**Key Points:**

- Important differences in precipitation recycling are found using water tracers embedded in a convection-permitting model (CPM) and a non-CPM
- The revised 2L-DRM simple moisture tracking model replicates the CPM's precipitation recycling estimates at a fraction of the cost
- We quantified the climatological moisture sources for precipitation over 15 South American regions using a CPM to drive the 2L-DRM

**Supporting Information:**

Supporting Information may be found in the online version of this article.

**Correspondence to:**

F. Dominguez,
francina@illinois.edu

**Citation:**

Claros, E., Dominguez, F., & Liu, C. (2025). Moisture sources of precipitation using convection-permitting simulations: A study over South America. *Geophysical Research Letters*, *52*, e2025GL118806. https://doi.org/10.1029/2025GL118806

Received 14 AUG 2025
Accepted 18 NOV 2025

**Author Contributions:**

**Conceptualization:** Erick Claros, Francina Dominguez
**Data curation:** Erick Claros, Changhai Liu
**Formal analysis:** Erick Claros
**Investigation:** Erick Claros
**Methodology:** Erick Claros, Francina Dominguez
**Software:** Erick Claros
**Supervision:** Francina Dominguez, Changhai Liu
**Validation:** Erick Claros
**Visualization:** Erick Claros
**Writing – original draft:** Erick Claros
**Writing – review & editing:** Erick Claros, Francina Dominguez, Changhai Liu

## Abstract

Climatological analyses of moisture sources of precipitation have traditionally relied on reanalyses or models that parameterize convection. Convection-permitting models (CPMs) are increasingly used in climate studies, as they better represent many precipitation processes than non-CPMs. We found significant differences in precipitation moisture sources over the Amazon Basin using 1-year CPM and non-CPM WRF simulations with moisture tracers. Notably, the CPM estimates that about half of precipitation in the central Andes comes from the Amazon basin; a 20%–30% higher estimate than the non-CPM. This suggests long-term CPMs with tracers could improve climatological estimates. However, their high computational cost is prohibitive. To overcome this, we developed a revised 2L-DRM model that replicates CPM-with-tracers estimates at a fraction of the cost, using only standard outputs. We applied this model to South America, analyzing precipitation moisture sources across 15 regions. 2L-DRM can be used for other regions as continental-scale CPM climatological simulations become available.

## Plain Language Summary

Quantifying moisture sources of precipitation is important for identifying critical dependencies of rainfall on evaporation from terrestrial and oceanic regions, especially in the context of climate and land use change. Climate models are a key tool for this, but most long-term studies have used models with coarse resolution that may miss important features. This study looks at convection-permitting models (CPMs), which simulate rainfall more realistically than traditional coarse models (non-CPMs). We compared CPM and non-CPM 1-year simulations with moisture tracking capabilities over the Amazon Basin. We found major differences in precipitation of local origin, especially in the Central Andes, where up to 50% of precipitation comes from Amazonian evaporation. While CPMs could improve our understanding of moisture sources, running long-term simulations to obtain climatological estimates is very expensive. To solve this, we updated a simpler model (2L-DRM) that provides similar results at a much lower computational cost. We then used this tool to study South America (2000–2021), estimating where rain in 15 regions comes from. This approach opens the door for better, more detailed climate-scale studies of precipitation moisture sources, without the need for high-cost tracers.

## 1. Introduction

Moisture tracking models are a popular numerical tool for quantifying the amount of precipitation over a target region that originates as evaporation from a source region, expressed as its ratio to total precipitation ($\rho$). When the target and source regions are the same, $\rho$ is known as the precipitation recycling ratio. These models have been used to study the origin of extreme precipitation and floods (Kim & Dominguez, 2023; Sodemann et al., 2009), to estimate continental evaporation's contribution to precipitation (Chug et al., 2022; Ent et al., 2010) and to identify feedbacks between deforestation, precipitation changes and drought (Nguyen et al., 2025; Ruiz-Vásquez et al., 2020; Staal et al., 2020; Zemp et al., 2017).

However, due to computational power limitations, climate studies using moisture-tracking models have relied on simulations and reanalysis products at coarse spatial resolutions, which are unable to represent convection, a key process in precipitation generation in many regions of the world (Nesbitt et al., 2006; Rajagopal et al., 2023). Coarse climate models rely on convection parameterizations that are a major source of uncertainties and errors (Brockhaus et al., 2008; Dai et al., 1999; Fosser et al., 2015; Jones & Randall, 2011; Karki et al., 2017; Prein et al., 2013; Zou et al., 2024). These include an incorrect diurnal precipitation cycle, too frequent light precipitation, and poor representation of precipitation extremes and spatial patterns.

Over the last decade, multi-decadal convection-permitting model (CPM) simulations at continental scales have emerged (Berthou et al., 2018; Leutwyler et al., 2016; Liu et al., 2017; R. M. Rasmussen et al., 2023; Stratton et al., 2018), offering several advantages such as improved representation of high-intensity precipitation and the diurnal cycle of precipitation. Recently, the South America Affinity Group (SAAG) developed a 22-year, 4-km CPM simulation (Dominguez et al., 2024), demonstrating that CPM simulations over South America outperform non-CPM simulations in reproducing several precipitation characteristics (Dominguez et al., 2024; Liu et al., 2025).

The natural next step is to use CPMs to analyze moisture sources of precipitation (Hu et al., 2024; Ma et al., 2024; Wallace & Minder, 2024; Wang et al., 2023; Yang et al., 2019). Our underlying assumption is that, similar to the case of precipitation, CPMs provide a more accurate representation of moisture sources of precipitation than non-CPMs. In this regard, Zou et al. (2024) found a 3% difference in spring precipitation recycling ratios ($\rho$) over the Tibetan Plateau using a bulk moisture model (Brubaker et al., 1993) forced with CPM and non-CPM data. However, the simplifying assumptions of bulk moisture models can introduce substantial errors (Dominguez et al., 2006; Fitzmaurice, 2007), which we avoid by comparing $\rho$s calculated directly using tracers embedded within CPM and non-CPM simulations.

The overarching goal of our work is to present the first continental-scale climatological analysis of sources and sinks of precipitation using a CPM. Our focus is South America. First, we demonstrate that moisture source calculations using a CPM are significantly different from those of a non-CPM. To do this, we obtain benchmark 1-year estimates of precipitation recycling over the Amazon Basin using the Weather Research Forecast model with water vapor tracers (WRF-WVT) in convection and non-convection permitting modes (Insua-Costa & Miguez-Macho, 2018). Since multi-decadal CPM WRF-WVT simulations are computationally unfeasible at continental scales, our second goal is to evaluate the computationally efficient 2L-DRM model (Dominguez et al., 2020) against the WRF-WVT CPM benchmark. Finally, we apply the validated 2L-DRM to estimate climate-scale moisture contributions across South America using SAAG's CPM outputs.

## 2. Materials and Methods

### 2.1. WRF-WVT Model

We use the WRF-WVT (Insua-Costa & Miguez-Macho, 2018), which incorporates water vapor tracers (WVTs) in the WRF model (version 4.3.3). WRF-WVT tags the moisture that evaporates from a specified source region and tracks it in space and time until it falls as precipitation. The tagged moisture undergoes the same physical processes as the total moisture: transport by the dynamical core and parameterizations for the planetary boundary layer (PBL), microphysics and convection (the convection parameterization is turned off in the CPM mode). The simulations were conducted over a spatial domain covering the Amazon Basin (Figure 1a) for one hydrological year (May 2018–May 2019). The first month (May 2018) was discarded to allow sufficient tracking time for reliable recycled precipitation estimates. The CPM simulation used a domain of 1,056 × 864 grid points with 4-km grid spacing, while the non-CPM simulation covered 176 × 144 grid points with 24-km grid spacing. Additional simulation details are provided in Text S1 of Supporting Information S1.

In addition to the standard WRF output variables, WRF-WVT also provides tracked precipitation ($P_{tr}$). We estimate the precipitation recycling ratio ($\rho$) by dividing $P_{tr}$ by the total precipitation ($P$). Given its detailed representation of physical processes, we treat the CPM WRF-WVT's precipitation recycling estimates as "truth" (Cloux et al., 2021; Crespo-Otero et al., 2024; Dominguez et al., 2020).

### 2.2. 2L-DRM Model

2L-DRM (Dominguez et al., 2020) is a moisture tracking model that estimates the fraction of precipitation that originates from evapotranspiration from defined source regions (i.e., $\rho$). Unlike the original DRM model (Dominguez et al., 2006), 2L-DRM divides the atmosphere into two slabs to capture wind trajectories at different atmospheric levels, which is crucial under strong wind shear (Goessling & Reick, 2013).

To calculate $\rho$ at a specific grid cell, slab, and time, the model first computes the backward wind trajectory. 2L-DRM estimates $\rho$ by calculating moisture contributions along this trajectory and then solving the moisture balance equation in time. Repeating this process for all grid cells, slabs, and time steps throughout the spatial and

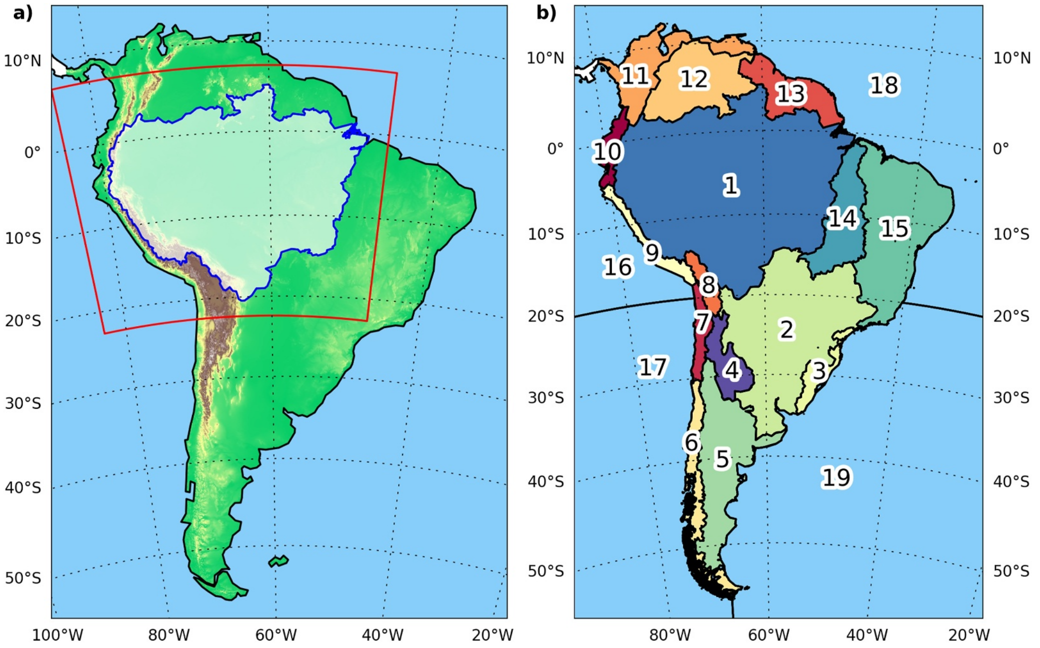

**Figure 1.** (a) WRF-WVT simulation domain (red rectangle) and source region (Amazon basin) delineated in blue. (b) 2L-DRM simulation domain over South America and defined source regions.

temporal domain, followed by spatial and temporal aggregation, the model obtains $\rho$ for the desired study area and time period.

### 2.2.1. Moisture Balance Equations

The 2L-DRM relies on the conservation of moisture within each of the two slabs. Recycled moisture is the moisture originating from the source region's evapotranspiration. The full derivation is provided in Text S2 of Supporting Information S1, here we present the final equations and numerical implementation.

Thus, the moisture conservation equation for the lower slab is:

$$\frac{d\rho_1}{dt} = \left(\rho_{\text{surf}} - \rho_1\right)\frac{E}{w_1} + \left(\rho_2 - \rho_1\right)\frac{F^d}{w_1} \tag{1}$$

Similarly, for the upper slab:

$$\frac{d\rho_2}{dt} = \left(\rho_1 - \rho_2\right)\frac{F^u}{w_2} \tag{2}$$

where $\rho_1$ and $\rho_2$ represent the recycling ratio in the lower and upper slabs, respectively. $E$ is the evapotranspiration, $\rho_{\text{surf}} = 1$ when $E$ is coming from the source region, and $\rho_{\text{surf}} = 0$ otherwise. $w_1$ and $w_2$ denote the precipitable water in each slab, while $F_u$ and $F_d$ are the upward and downward moisture fluxes between slabs, respectively. If the vertical wind direction is upward (downward), then $F^u > 0$ $\left(F^d > 0\right)$ and $F^d = 0$ $(F^u = 0)$.

Using the total derivative in Equations 1 and 2 allows us to directly apply these equations along the 2L-DRM trajectories.

### 2.2.2. Numerical Implementation

To ensure realistic $\rho$ values $(0 \le \rho \le 1)$ by controlling numerical instabilities, here we discretize Equations 1 and 2 using finite differences and Euler's method. Using the superscripts $n$ and $n + 1$ for denoting consecutive time steps, we discretize Equation 1 as:

$$\frac{\rho_1^{n+1}-\rho_1^n}{\Delta t} = \left(\rho_{\text{surf}}^n-\rho_1^n\right)\frac{E^n}{w_1^n}+\left(\rho_2^n-\rho_1^n\right)\frac{F^{d,n}}{w_1^n}$$

$$\rho_1^{n+1} = \rho_1^n+\left(\rho_{\text{surf}}^n-\rho_1^n\right)\frac{E^n\Delta t}{w_1^n}+\left(\rho_2^n-\rho_1^n\right)\frac{F^{d,n}\Delta t}{w_1^n} \tag{3}$$

Similarly, for Equation 2 (upper slab), we obtain:

$$\rho_2^{n+1} = \rho_2^n+\left(\rho_1^n-\rho_2^n\right)\frac{F^{u,n}\Delta t}{w_2^n} \tag{4}$$

From Equations 3 and 4, we observe that for calculating $\rho_1$ we require previous values of $\rho_2$ and vice-versa. Thus, similarly to (Dominguez et al., 2020), when we follow a trajectory in the lower slab (upper slab), we assume that the same trajectory occurs in the upper slab (lower slab), which allows us to obtain all the required $\rho_1$ and $\rho_2$ values by jointly calculating Equations 3 and 4. Furthermore, we assume that at the beginning of the trajectory $\rho_1^0 = 0$ and $\rho_2^0 = 0$. By calculating iteratively for all time steps in the trajectory, we obtain the desired $\rho_1$ and $\rho_2$ values at the end of the trajectory (see Text S3 in Supporting Information S1 for details on numerical implementation).

The solution presented here differs from that proposed by Dominguez et al. (2020) in the way Equations 1 and 2 are solved. While their approach was based on an analytical solution to these equations, here we directly apply a numerical discretization. Therefore, the current 2L-DRM version is no longer an analytical model, but can be classified as an offline model, following the moisture tracking model classification of Dominguez et al. (2020). However, when analyzing the lower (or upper) slab we still assume identical trajectories in the opposite slab, a major weakness of the model implementation.

### 2.2.3. Computational Efficiency

While WRF-WVT provides highly reliable estimates of precipitation recycling due to its physical realism, it is computationally expensive, especially at CPM resolutions. With the recent emergence of standard CPM climate simulations (i.e., without water vapor tracers), the 2L-DRM offers a much cheaper alternative for calculating precipitation recycling and moisture contributions using these readily available data sets.

For instance, running the WRF-WVT CPM 1-year simulation over the Amazon Basin required 130 wall-clock hours on 2,048 cores. In contrast, the 2L-DRM completed the 1-year simulation in just 1.6 wall-clock hours using 128 cores. Thus, the 2L-DRM can be run at a fraction of the computational cost (0.077%) of WRF-WVT. Another key advantage of the 2L-DRM is that it allows tracking multiple source regions simultaneously within a single simulation, unlike WRF-WVT, which requires a separate simulation for each source region.

### 2.2.4. 2L-DRM Simulation Over the Amazon Basin

To capture wind differences induced by the Andes and to avoid numerical instabilities due to the interface between slabs potentially intersecting the topography, 500 hPa was chosen as the pressure level dividing the two slabs. We calculate the required 2L-DRM inputs at a 3-hr temporal resolution using standard WRF outputs from the WRF-WVT simulation. The 2L-DRM is then run using the same source region and analysis period as the WRF-WVT simulation. Trajectories are initialized every 3 hr and are back-tracked with a tracing time step of 15 min until they either leave the domain or reach a maximum duration of 15 days. The 15-day limit was chosen based on the global mean water residence time of 8.9 days with a standard deviation of 0.4 days (van der Ent & Tuinenburg, 2017).

Importantly, since the calculation of inputs relies solely on standard WRF output variables and does not require the special tracer outputs from WRF-WVT, this procedure replicates the results that would be obtained by applying the 2L-DRM to a standard WRF simulation, making the $\rho$ estimates from WRF-WVT and 2L-DRM directly comparable.

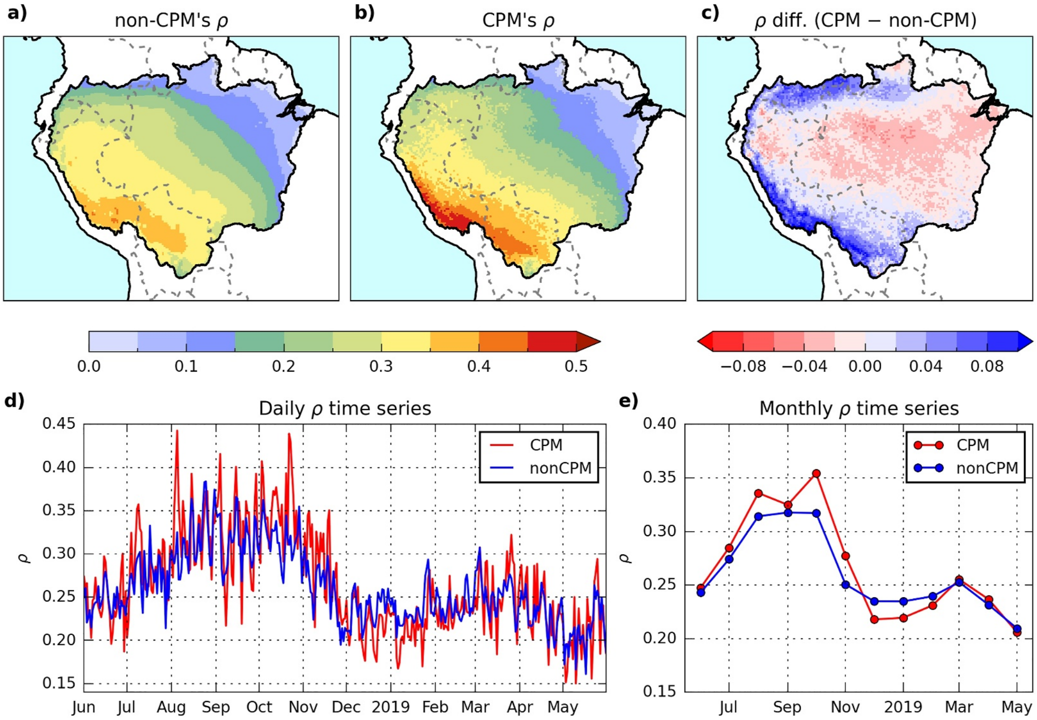

**Figure 2.** WRF-WVT CPM and non-CPM $\rho$ estimates for the Amazon Basin: hydrological year (June 2018–May 2019) estimates from the CPM (a) and non-CPM simulation (b), their difference (c), and daily (d) and monthly (e) time series.

### 2.2.5. 2L-DRM Simulation Over South America

Using a similar procedure as described in 2.2.4, we compute the 2L-DRM inputs from the SAAG simulation data (Dominguez et al., 2024). It is important to emphasize that the SAAG simulation does not have numerical water tracers. A key difference in this case is that we use multiple source regions, instead of considering only the Amazon Basin. The 19 source regions used (Figure 1b) are defined based on South America's main basins (15 continental regions) and a north–south division of the Pacific and Atlantic Oceans (4 oceanic regions).

## 3. Results and Discussion

### 3.1. Differences Between CPM and Non-CPM Precipitation Recycling

Both the CPM and non-CPM WRF-WVT simulations show a gradual increase in precipitation recycling over the Amazon Basin toward the southwest (Figures 2a and 2b), which is consistent with previous studies (Dominguez et al., 2022; Yang & Dominguez, 2019). Moreover, the highest precipitation recycling occurs during the dry season (Aug–Oct) for both the CPM (0.35) and non-CPM (0.32), while the minimum occurs in May (0.2 for both cases) (Figure 2e).

There are some critical differences between the precipitation recycling calculated using the CPM and non-CPM simulations. Although both have a similar overall $\rho$ (0.254 for the non-CPM and 0.256 for the CPM case), there are marked differences in how $\rho$ is spatially distributed (Figures 2a–2c). This is most evident over the Central Andes, where $\rho$ increases by approximately 0.08–0.1 (an increase of 20%–30%) in the CPM simulation. The CPM simulation highlights the dependence of Central Andes precipitation on evaporation from the Amazon Basin—indicating that 40%–50% of the precipitation is derived from Amazonian evaporation. Furthermore, when examining the seasonal scale (Figure S1 in Supporting Information S1), we observe that this critical dependence is consistent across all seasons, increasing confidence that this feature is inherent to the CPM's climate representation, although only 1 year is evaluated. Moreover, SON shows particularly pronounced differences, with markedly higher CPM $\rho$ further extending into the lowlands adjacent to the Andes and covering nearly half of the Amazon Basin.

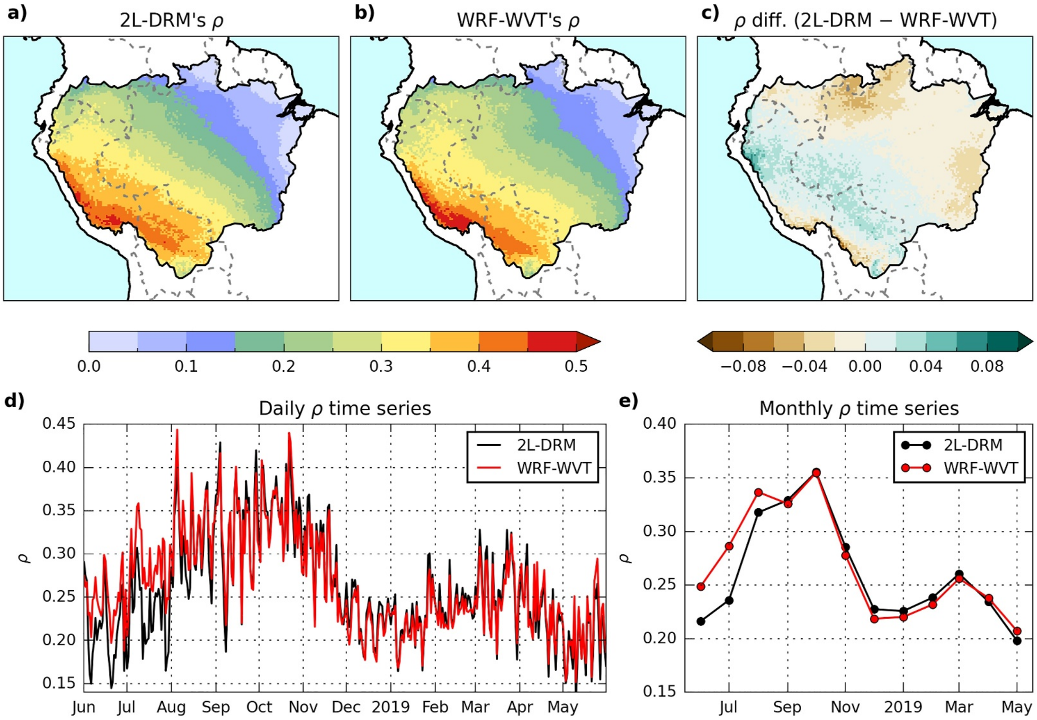

**Figure 3.** WRF-WVT CPM and 2L-DRM $\rho$ estimates for the Amazon Basin: hydrological year (June 2018–May 2019) estimates from 2L-DRM (a) and WRF-WVT CPM (b), their difference (c), and daily (d) and monthly (e) time series.

We also observe higher $\rho$ values for the CPM simulation in the northwest region (Figure 2c), and lower values in the central and eastern part of the Amazon basin. At the daily timescale (Figure 2d), the CPM simulation shows greater variability in $\rho$ throughout the year, exhibiting both higher and lower values than the non-CPM simulation during similar periods. On the other hand, both the CPM and non-CPM cases show a similar seasonality (Figures 2d and 2e). However, the CPM slightly emphasizes this seasonality, with lower $\rho$s during December-February and higher $\rho$s during August–November (differences up to 0.04). Since only one hydrological year is analyzed, a longer simulation comparison period would be required to confirm this.

These differences may be partially explained by the closer agreement of the CPM-simulated precipitation with observations (Text S4 in Supporting Information S1). The CPM simulation estimates less precipitation than the non-CPM, except over the Central Andes. While some hypotheses can be derived, further analysis is required to fully understand the underlying mechanisms driving the differences in recycling. Nevertheless, we can conclude from our results that there are significant differences, and they are particularly critical for regions such as the Central Andes.

### 3.2. WRF-WVT Versus 2L-DRM

The previous analysis revealed that precipitation recycling estimates derived from WRF-WVT simulations without convective parameterizations (CPM) are different from those with parameterized convection. However, running WRF-WVT at convection-resolving scales for climate timescales is computationally unfeasible. Therefore, in this section, we investigate whether similar results can be obtained using the simpler and more cost-efficient 2L-DRM, which can use the outputs from standard CPM simulations that are more widely available. Thus, we compare the WRF-WVT CPM's $\rho$ estimates with those obtained from running 2L-DRM.

Figures 3a and 3b shows that the 2L-DRM model captures the general spatial pattern and strong dependence of the Central Andes on precipitation recycling, although the values are slightly lower than those from the WRF-WVT. The 2L-DRM tends to slightly underestimate $\rho$ in the eastern Amazon and the slopes of the central Andes, while $\rho$ in the western Amazon is slightly overestimated. Furthermore, Figure 3 shows that the majority of $\rho$ differences fall between −0.02 and 0.02, with only small isolated regions outside this range. Therefore, we can consider that differences at the annual scale are minimal. Moreover, when we look at the $\rho$ time series, we observe a very similar temporal pattern across all months, except in June and July. However, the larger differences in these months could be impacted by model initialization.

On the other hand, an important feature of the 2L-DRM is that it can reproduce the daily variability of $\rho$ (Figure 3d), except during the first 2 months of the simulation, when it underestimates $\rho$. A similar pattern is seen in the monthly time series (Figure 3e). In addition, the overall annual $\rho$ for the Amazon basin is correctly estimated by the 2LDRM model (0.254), when compared to the WRF-WVT (0.256). From this comparison, we conclude that the 2L-DRM model captures the key features of the WRF-WVT CPM simulation remarkably well, given the important simplifications of the 2L-DRM model.

## 3.3. Application to South America

### 3.3.1. Source Regions: Contribution to Precipitation Over South America

We now calculate the moisture contribution from different South American regions using the 2L-DRM applied to the 22-year SAAG's WRF CPM simulation data set. Figure 4 (regions 1–15) shows the contribution of the continental regions to precipitation over South America. The Amazon Basin contributes an important fraction of moisture to precipitation over adjacent areas, especially over the western flank of the Andes and near the border with the La Plata Basin. This highlights the key role of the Amazon Basin as a moisture source for precipitation in South America. In contrast, despite their size, the southernmost regions (regions 5 and 6) contribute very little to precipitation, even within their own areas. The La Plata, Orinoco and Altiplano regions (2, 12, 8) are also important moisture sources for the continent.

Figure 4 (regions 16–19) highlights the importance of oceanic source regions. The North Atlantic and South Pacific Oceans contribute significantly to rainfall in adjacent areas, while the South Atlantic and North Pacific have minimal impact. Furthermore, it is important to note that this subsection describes annual averages, but values can vary seasonally (Figure S5 in Supporting Information S1).

### 3.3.2. Continental Regions: Moisture Sources of Precipitation

Figure 5a shows the dependence of precipitation over the 15 continental regions on evaporation from the 19 regions analyzed. We observe that the Amazon Basin's evaporation approximately accounts for 1/3 of the precipitation over the Central Pacific Basin (region 9) and 1/4 over the Altiplano (region 8), reaching values as high as 0.42 and 0.31, respectively, during DJF (Figure S8 in Supporting Information S1). This indicates that, despite the blocking effect of the mountains, moisture from the Amazon Basin is crucial for precipitation on the western side of the Andes. This is emphasized by noticing that these fractions are comparable to or even higher than the Amazon Basin's own recycling ratio (~1/4), and that the continental evaporation contribution to precipitation is roughly 0.5 in these regions (Figure 5b). However, the complex topography may affect estimates of moisture transported across the Andes, so further analysis is required.

The La Plata Basin is another important moisture provider, contributing nearly 1/5 of the precipitation over regions 3 (Eastern coast to La Plata) and 4 (Southern Andean endorheic basins). Meanwhile, evaporation from the North Atlantic Ocean accounts for nearly 1/3 of the precipitation in region 13 (Guyanas) and 1/4 in region 12 (Orinoco Basin). Additionally, nearly 1/5 of the precipitation over region 6 (Southern Pacific Basin) and region 7 (Atacama) originates as evaporation from the South Pacific Ocean.

Figure 5b summarizes the recycling ratios for the continental regions. While recycling over the Amazon and La Plata basins accounts for nearly 1/4 and 1/5 of precipitation, respectively, it is remarkable that, despite its small size, the Altiplano has a high recycling ratio (0.18). This highlights the importance of local evaporation in sustaining precipitation over the Altiplano and, as suggested by the hotspot in Figure 4, is likely related to Lake Titicaca's effect on evaporation and convection (Llacza et al., 2025). Furthermore, the Amazon Basin's recycling ratio (0.26) closely matches the 1-year WRF-WVT CPM estimate (0.25) but is now derived from a 22-year analysis. This value lies at the lower end of previous estimates (Figure 1 in Dominguez et al., 2022), which use a variety of models and consistently estimate recycling to be between 25% and 35%.

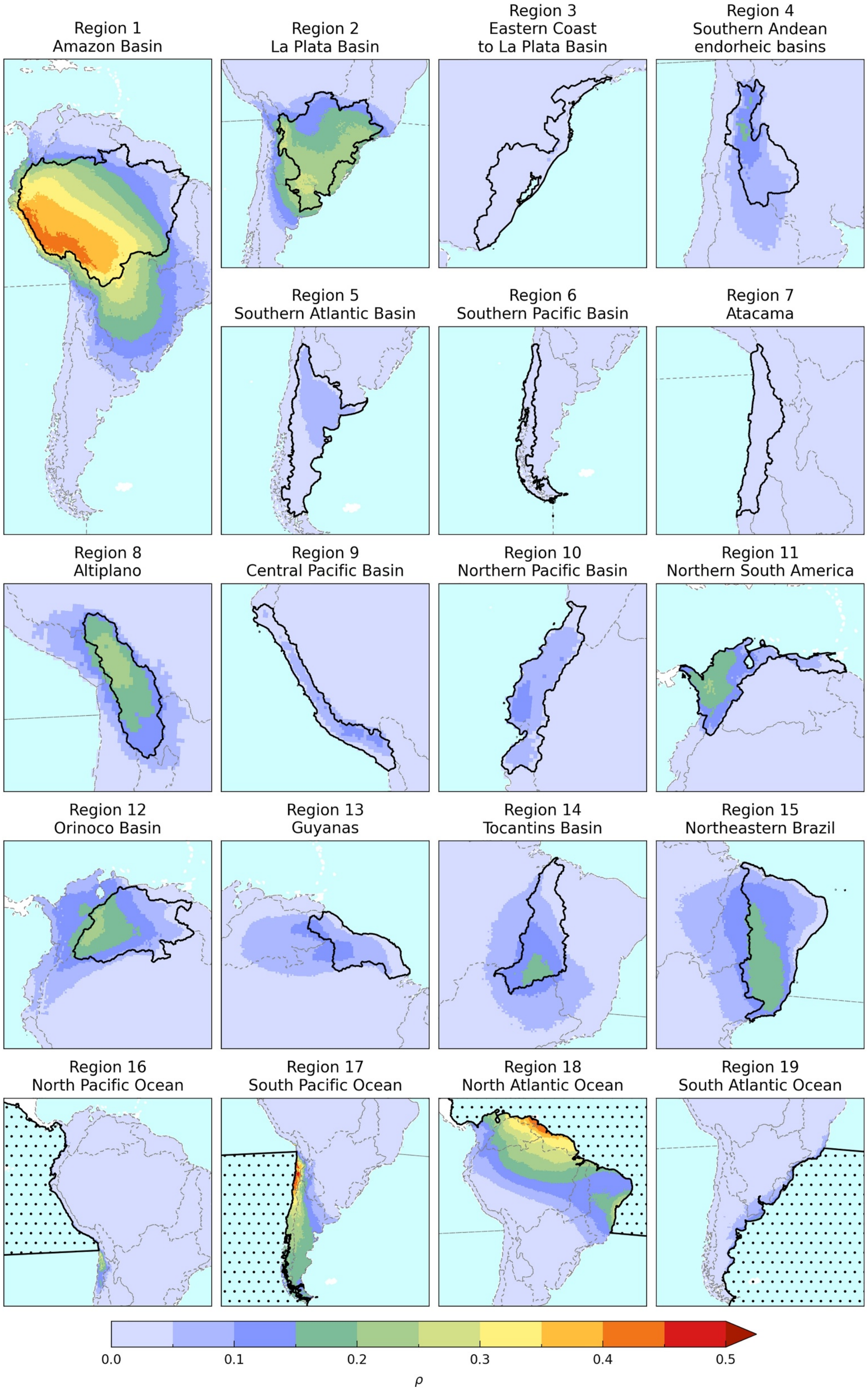

**Figure 4.** Fraction of precipitation originating as evaporation from source regions ($\rho$). Each map shows a different source region (outlined in black). Oceanic source regions are additionally filled with dots.

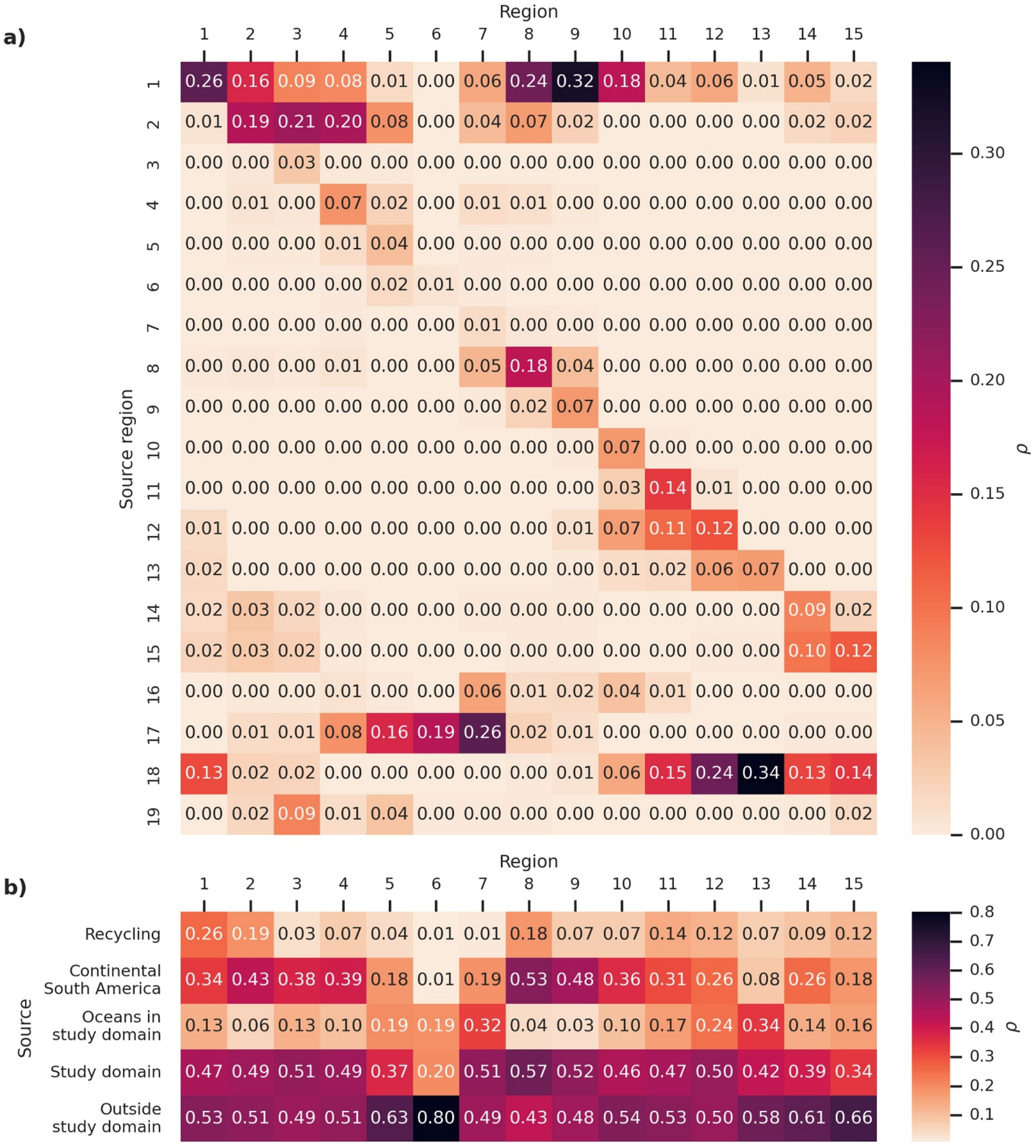

a)

| Source region \ Region | 1 | 2 | 3 | 4 | 5 | 6 | 7 | 8 | 9 | 10 | 11 | 12 | 13 | 14 | 15 |
|---|---|---|---|---|---|---|---|---|---|---|---|---|---|---|---|
| 1 | 0.26 | 0.16 | 0.09 | 0.08 | 0.01 | 0.00 | 0.06 | 0.24 | 0.32 | 0.18 | 0.04 | 0.06 | 0.01 | 0.05 | 0.02 |
| 2 | 0.01 | 0.19 | 0.21 | 0.20 | 0.08 | 0.00 | 0.04 | 0.07 | 0.02 | 0.00 | 0.00 | 0.00 | 0.00 | 0.02 | 0.02 |
| 3 | 0.00 | 0.00 | 0.03 | 0.00 | 0.00 | 0.00 | 0.00 | 0.00 | 0.00 | 0.00 | 0.00 | 0.00 | 0.00 | 0.00 | 0.00 |
| 4 | 0.00 | 0.01 | 0.00 | 0.07 | 0.02 | 0.00 | 0.01 | 0.01 | 0.00 | 0.00 | 0.00 | 0.00 | 0.00 | 0.00 | 0.00 |
| 5 | 0.00 | 0.00 | 0.00 | 0.01 | 0.04 | 0.00 | 0.00 | 0.00 | 0.00 | 0.00 | 0.00 | 0.00 | 0.00 | 0.00 | 0.00 |
| 6 | 0.00 | 0.00 | 0.00 | 0.00 | 0.02 | 0.01 | 0.00 | 0.00 | 0.00 | 0.00 | 0.00 | 0.00 | 0.00 | 0.00 | 0.00 |
| 7 | 0.00 | 0.00 | 0.00 | 0.00 | 0.00 | 0.00 | 0.01 | 0.00 | 0.00 | 0.00 | 0.00 | 0.00 | 0.00 | 0.00 | 0.00 |
| 8 | 0.00 | 0.00 | 0.00 | 0.01 | 0.00 | 0.00 | 0.05 | 0.18 | 0.04 | 0.00 | 0.00 | 0.00 | 0.00 | 0.00 | 0.00 |
| 9 | 0.00 | 0.00 | 0.00 | 0.00 | 0.00 | 0.00 | 0.00 | 0.02 | 0.07 | 0.00 | 0.00 | 0.00 | 0.00 | 0.00 | 0.00 |
| 10 | 0.00 | 0.00 | 0.00 | 0.00 | 0.00 | 0.00 | 0.00 | 0.00 | 0.00 | 0.07 | 0.00 | 0.00 | 0.00 | 0.00 | 0.00 |
| 11 | 0.00 | 0.00 | 0.00 | 0.00 | 0.00 | 0.00 | 0.00 | 0.00 | 0.00 | 0.03 | 0.14 | 0.01 | 0.00 | 0.00 | 0.00 |
| 12 | 0.01 | 0.00 | 0.00 | 0.00 | 0.00 | 0.00 | 0.00 | 0.00 | 0.01 | 0.07 | 0.11 | 0.12 | 0.00 | 0.00 | 0.00 |
| 13 | 0.02 | 0.00 | 0.00 | 0.00 | 0.00 | 0.00 | 0.00 | 0.00 | 0.00 | 0.01 | 0.02 | 0.06 | 0.07 | 0.00 | 0.00 |
| 14 | 0.02 | 0.03 | 0.02 | 0.00 | 0.00 | 0.00 | 0.00 | 0.00 | 0.00 | 0.00 | 0.00 | 0.00 | 0.00 | 0.09 | 0.02 |
| 15 | 0.02 | 0.03 | 0.02 | 0.00 | 0.00 | 0.00 | 0.00 | 0.00 | 0.00 | 0.00 | 0.00 | 0.00 | 0.00 | 0.10 | 0.12 |
| 16 | 0.00 | 0.00 | 0.00 | 0.01 | 0.00 | 0.00 | 0.06 | 0.01 | 0.02 | 0.04 | 0.01 | 0.00 | 0.00 | 0.00 | 0.00 |
| 17 | 0.00 | 0.01 | 0.01 | 0.08 | 0.16 | 0.19 | 0.26 | 0.02 | 0.01 | 0.00 | 0.00 | 0.00 | 0.00 | 0.00 | 0.00 |
| 18 | 0.13 | 0.02 | 0.02 | 0.00 | 0.00 | 0.00 | 0.00 | 0.00 | 0.01 | 0.06 | 0.15 | 0.24 | 0.34 | 0.13 | 0.14 |
| 19 | 0.00 | 0.02 | 0.09 | 0.01 | 0.04 | 0.00 | 0.00 | 0.00 | 0.00 | 0.00 | 0.00 | 0.00 | 0.00 | 0.00 | 0.02 |

b)

| Source \ Region | 1 | 2 | 3 | 4 | 5 | 6 | 7 | 8 | 9 | 10 | 11 | 12 | 13 | 14 | 15 |
|---|---|---|---|---|---|---|---|---|---|---|---|---|---|---|---|
| Recycling | 0.26 | 0.19 | 0.03 | 0.07 | 0.04 | 0.01 | 0.01 | 0.18 | 0.07 | 0.07 | 0.14 | 0.12 | 0.07 | 0.09 | 0.12 |
| Continental South America | 0.34 | 0.43 | 0.38 | 0.39 | 0.18 | 0.01 | 0.19 | 0.53 | 0.48 | 0.36 | 0.31 | 0.26 | 0.08 | 0.26 | 0.18 |
| Oceans in study domain | 0.13 | 0.06 | 0.13 | 0.10 | 0.19 | 0.19 | 0.32 | 0.04 | 0.03 | 0.10 | 0.17 | 0.24 | 0.34 | 0.14 | 0.16 |
| Study domain | 0.47 | 0.49 | 0.51 | 0.49 | 0.37 | 0.20 | 0.51 | 0.57 | 0.52 | 0.46 | 0.47 | 0.50 | 0.42 | 0.39 | 0.34 |
| Outside study domain | 0.53 | 0.51 | 0.49 | 0.51 | 0.63 | 0.80 | 0.49 | 0.43 | 0.48 | 0.54 | 0.53 | 0.50 | 0.58 | 0.61 | 0.66 |

**Figure 5.** Fraction of precipitation in continental regions (columns) originating as evaporation from source regions (rows). (a) shows the source-sink estimates from the predefined 19 source regions. (b) shows the local recycling (source and sink regions are the same) (row 1), summation of all sources from continental South America (regions 1–15) (row 2), summation of all sources from oceans in study domain (regions 16–19) (row 3), study domain or summation of continental and oceanic sources (row 4) and outside study domain (row 5).

Figure 5b also shows that continental evaporation can explain nearly half of the precipitation in the Altiplano and Central Pacific Basin, while it is irrelevant in the South Pacific Basin ($\rho = 0.01$). Seasonal estimates are presented in Figures S6–S9 of Supporting Information S1.

## 4. Conclusions

We show that important differences arise in precipitation recycling estimates over the Amazon Basin when using a CPM versus a non-CPM. Based on a 1-year WRF-WVT simulation over the Amazon Basin, we found that 8%–10% more total precipitation over the Central Andes is explained by the Amazon Basin recycling process in the CPM case—corresponding to a 20%–30% increase in the recycling ratio. Thus, the CPM highlights the critical dependence of the Central Andes precipitation—nearly 50%—on Amazonian evaporation.

However, obtaining climatological estimates of precipitation recycling by running a CPM with tracers is computationally unfeasible. Therefore, we propose as alternative a revised version of the 2L-DRM, which is computationally much cheaper and can be driven by standard CPM outputs that are already available for several regions. When tested using standard WRF outputs from the WRF-WVT simulation over the Amazon, the 2L-DRM was able to capture the key features of the CPM's precipitation recycling estimates. Critically, the 2L-DRM operated at a fraction of the computational cost—just 0.077%—of the WRF-WVT.

Finally, we presented climatological estimates of the moisture sources for precipitation in the major South American basins using the 2L-DRM driven by the SAAG CPM data. The results highlight the importance of the Amazon Basin as a moisture provider for precipitation, especially on the western flank of the Andes, with Amazonian contributions as high as $\rho = 1/3$ in the Central Pacfic Basin and $\rho = 1/4$ in the Altiplano. While the highest precipitation recycling ratios correspond to the Amazon ($\rho = 0.26$) and La Plata Basin ($\rho = 0.19$), it is remarkable that, despite its small size, the Altiplano has a $\rho = 0.18$, which emphasizes the importance of local evaporation for precipitation over this region. Moreover, among the oceanic sources analyzed, the North Atlantic and South Pacific are the most important in terms of moisture contributions, while the South Atlantic and North Pacific Oceans have a minimal effect.

As CPM simulations become available throughout the globe, it will be important to revisit existing calculations of moisture sources and sinks that inherited the errors of convective parameterizations. Prior estimates of moisture sources are likely to be most affected in regions where precipitation is dependent on mesoscale or orographic processes (Prein et al., 2021; R. Rasmussen et al., 2011), and in other regions where precipitation recycling strongly sustains rainfall, such as the Congo Basin (Sorí et al., 2022; Tuinenburg et al., 2020; Worden et al., 2021). Critically, CPM simulations will become a key tool to understand the effect of land use and land cover (LULC) change on continental hydroclimates, revealing the effect of mesoscale land surface heterogeneity on the overlying atmosphere in a way that non-CPM simulations have not been able to resolve. As such, computationally efficient and robust tools, such as 2L-DRM, can help us analyze the vast amounts of newly available CPM data, understand the physical mechanisms that affect precipitation, and disentangle the role of moisture recycling in simulations with LULC change.

## Conflict of Interest

The authors declare no conflicts of interest relevant to this study.

## Data Availability Statement

The 2L-DRM outputs for South America are available at (Claros et al., 2025a), facilitating more detailed analyses and enabling the study of target regions different from those studied in this work. The 2L-DRM source code is available on GitHub (Claros et al., 2025b). A preprocessing tool to obtain 2L-DRM inputs from WRF outputs is also provided on GitHub (Claros et al., 2025c). The WRF-WVT model (Insua-Costa & Miguez-Macho, 2018) is available at: https://github.com/damianinsua/WRF-WVTs.git. The SAAG simulation outputs can be accessed via (R. M. Rasmussen et al., 2022), and ERA5 data is available at (European Centre for Medium-Range Weather Forecasts, 2019).

**Acknowledgments**
This research has been supported by PRONABEC (RJ 1954–2023). NCAR provided computational resources. Dominguez funded by NSF-AGS 1852709. We thank Professor Brian Jewett for his valuable feedback.

## References

Berthou, S., Kendon, E. J., Chan, S. C., Ban, N., Leutwyler, D., Schär, C., & Fosser, G. (2018). Pan-European climate at convection-permitting scale: A model intercomparison study. *Climate Dynamics 2018*, *55*(55), 35–59. https://doi.org/10.1007/S00382-018-4114-6

Brockhaus, P., Lüthi, D., & Schär, C. (2008). Aspects of the diurnal cycle in a regional climate model. *Meteorologische Zeitschrift*, *17*(4), 433–443. https://doi.org/10.1127/0941-2948/2008/0316

Brubaker, K. L., Entekhabi, D., & Eagleson, P. S. (1993). Estimation of continental precipitation recycling. *Journal of Climate*, *6*(6), 1077–1089. https://doi.org/10.1175/1520-0442(1993)006⟨1077:EOCPR⟩2.0.CO;2

Chug, D., Dominguez, F., & Yang, Z. (2022). The Amazon and la Plata river basins as moisture sources of South America: Climatology and intraseasonal variability. *Journal of Geophysical Research: Atmospheres*, *127*(12), e2021JD035455. https://doi.org/10.1029/2021JD035455

Claros, E., Dominguez, F., & Liu, C. (2025a). Dataset of moisture sources of precipitation using convection-permitting simulations: A study over South America [Dataset]. *Zenodo*. https://doi.org/10.5281/zenodo.17336564

Claros, E., Dominguez, F., & Liu, C. (2025b). Moisture tracking model 2L-DRM (v0.1.0) [Software]. *Zenodo*. https://doi.org/10.5281/zenodo.17337767

Claros, E., Dominguez, F., & Liu, C. (2025c). Preprocessing tool for the 2L-DRM model [Software]. *Zenodo*. https://doi.org/10.5281/zenodo.17382988

Cloux, S., Garaboa-Paz, D., Insua-Costa, D., Miguez-Macho, G., & Pérez-Muñuzuri, V. (2021). Extreme precipitation events in the Mediterranean area: Contrasting two different models for moisture source identification. *Hydrology and Earth System Sciences*, *25*(12), 6465–6477. https://doi.org/10.5194/hess-25-6465-2021

Crespo-Otero, A., Insua-Costa, D., Hernández-García, E., López, C., & Míguez-Macho, G. (2024). Simple physics-based adjustments reconcile the results of Eulerian and Lagrangian techniques for moisture tracking. *Earth System Dynamics Discussions*, *2024*, 1–25. https://doi.org/10.5194/esd-2024-18

Dai, A., Giorgi, F., & Trenberth, K. E. (1999). Observed and model-simulated diurnal cycles of precipitation over the contiguous United States. *Journal of Geophysical Research*, *104*(D6), 6377–6402. https://doi.org/10.1029/98JD02720

Dominguez, F., Eiras-Barca, J., Yang, Z., Bock, D., Nieto, R., & Gimeno, L. (2022). Amazonian moisture recycling revisited using WRF with water vapor tracers. *Journal of Geophysical Research: Atmospheres*, *127*(4), e2021JD035259. https://doi.org/10.1029/2021JD035259

Dominguez, F., Hu, H., & Martinez, J. A. (2020). Two-layer Dynamic Recycling Model (2l-DRM): Learning from moisture tracking models of different complexity. *Journal of Hydrometeorology*, *21*(1), 3–16. https://doi.org/10.1175/JHM-D-19-0101.1

Dominguez, F., Kumar, P., Liang, X.-Z., & Ting, M. (2006). Impact of atmospheric moisture storage on precipitation recycling. *Journal of Climate*, *19*(8), 1513–1530. https://doi.org/10.1175/JCLI3691.1

Dominguez, F., Rasmussen, R., Liu, C., Ikeda, K., Prein, A., Varble, A., et al. (2024). Advancing south American water and climate science through multidecadal convection-permitting modeling. *Bulletin of the American Meteorological Society*, *105*(1), E32–E44. https://doi.org/10.1175/BAMS-D-22-0226.1

Ent, R. J. V. D., Savenije, H. H., Schaefli, B., & Steele-Dunne, S. C. (2010). Origin and fate of atmospheric moisture over continents. *Water Resources Research*, *46*(9). https://doi.org/10.1029/2010WR009127

European Centre for Medium-Range Weather Forecasts. (2019). ERA5 reanalysis (0.25 degree latitude-longitude grid) [Dataset]. https://doi.org/10.5065/BH6N-5N20

Fitzmaurice, J. A. (2007). *A critical analysis of bulk precipitation recycling models*. Doctoral Dissertation. Massachusetts Institute of Technology. Retrieved from http://hdl.handle.net/1721.1/39356

Fosser, G., Khodayar, S., & Berg, P. (2015). Benefit of convection permitting climate model simulations in the representation of convective precipitation. *Climate Dynamics*, *44*, 45–60. https://doi.org/10.1007/S00382-014-2242-1/FIGURES/9

Goessling, H. F., & Reick, C. H. (2013). On the "well-mixed" assumption and numerical 2-D tracing of atmospheric moisture. *Atmospheric Chemistry and Physics*, *13*(11), 5567–5585. https://doi.org/10.5194/ACP-13-5567-2013

Hu, H., Leung, L. R., Feng, Z., & Marquis, J. (2024). Moisture recycling through pumping by mesoscale convective systems. *Journal of Hydrometeorology*, *25*(6), 867–880. https://doi.org/10.1175/jhm-d-23-0174.1

Insua-Costa, D., & Miguez-Macho, G. (2018). A new moisture tagging capability in the weather research and forecasting model: Formulation, validation and application to the 2014 great lake-effect snowstorm. *Earth System Dynamics*, *9*(1), 167–185. https://doi.org/10.5194/esd-9-167-2018

Jones, T. R., & Randall, D. A. (2011). Quantifying the limits of convective parameterizations. *Journal of Geophysical Research*, *116*(D8), 8210. https://doi.org/10.1029/2010JD014913

Karki, R., ul Hasson, S., Gerlitz, L., Schickhoff, U., Scholten, T., & Böhner, J. (2017). Quantifying the added value of convection-permitting climate simulations in complex terrain: A systematic evaluation of WRF over the Himalayas. *Earth System Dynamics*, *8*(3), 507–528. https://doi.org/10.5194/esd-8-507-2017

Kim, S. U., & Dominguez, F. (2023). Warm season extreme flood events in the midwestern us—sources of moisture and physical mechanisms. *Journal of Geophysical Research: Atmospheres*, *128*(14), e2022JD038208. https://doi.org/10.1029/2022JD038208

Leutwyler, D., Fuhrer, O., Lapillonne, X., Lüthi, D., & Schär, C. (2016). Towards European-scale convection-resolving climate simulations with GPUs: A study with COSMO 4.19. *Geoscientific Model Development*, *9*, 3393–3412. https://doi.org/10.5194/GMD-9-3393-2016

Liu, C., Ikeda, K., Prein, A., Scaff, L., Dominguez, F., Rasmussen, R., et al. (2025). Convection-permitting climate simulations over South America: Experimentation during different phases of ENSO. *Atmospheric Research*, *316*, 107936. https://doi.org/10.1016/j.atmosres.2025.107936

Liu, C., Ikeda, K., Rasmussen, R., Barlage, M., Newman, A. J., Prein, A. F., et al. (2017). Continental-scale convection-permitting modeling of the current and future climate of North America. *Climate Dynamics*, *49*(1–2), 71–95. https://doi.org/10.1007/s00382-016-3327-9

Llacza, A., Paredes, J., Llamocca, J., Saavedra, M., Fita, L., Ruiz, C., & Junquas, C. (2025). Improved spatial representation of precipitation and air surface temperature over highlands of the southern tropical Andes (Lake Titicaca region) during an Austral summer using the WRF model. *Atmospheric Research*, *325*, 108262. https://doi.org/10.1016/j.atmosres.2025.108262

Ma, M., Tang, J., Ou, T., & Chen, D. (2024). Contribution of recycled and external advected moisture to precipitation and its inter-annual variation over the Tibetan Plateau. *Journal of Geophysical Research: Atmospheres*, *129*(10), e2023JD040230. https://doi.org/10.1029/2023jd040230

Nesbitt, S. W., Cifelli, R., & Rutledge, S. A. (2006). Storm morphology and rainfall characteristics of TRMM precipitation features. *Monthly Weather Review*, *134*(10), 2702–2721. https://doi.org/10.1175/mwr3200.1

Nguyen, K., Hauser, L. T., Tuinenburg, O. A., Damm, A., & Santos, M. J. (2025). Deforestation-induced immediate and delayed shifts in moisture recycling: Source and sink dynamics across the Amazon. *Environmental Research Letters*, *20*(10), 104014. https://doi.org/10.1088/1748-9326/ADFD75

Prein, A. F., Gobiet, A., Suklitsch, M., Truhetz, H., Awan, N. K., Keuler, K., & Georgievski, G. (2013). Added value of convection permitting seasonal simulations. *Climate Dynamics*, *41*, 2655–2677. https://doi.org/10.1007/S00382-013-1744-6/FIGURES/13

Prein, A. F., Rasmussen, R. M., Wang, D., & Giangrande, S. E. (2021). Sensitivity of organized convective storms to model grid spacing in current and future climates. *Philosophical Transactions of the Royal Society A: Mathematical, Physical and Engineering Sciences*, *379*(2195), 20190546. https://doi.org/10.1098/rsta.2019.0546

Rajagopal, M., Russell, J., Skok, G., & Zipser, E. (2023). Tracking mesoscale convective systems in imerg and regional variability of their properties in the tropics. *Journal of Geophysical Research: Atmospheres*, *128*(24), e2023JD038563. https://doi.org/10.1029/2023jd038563

Rasmussen, R., Liu, C., Ikeda, K., Gochis, D., Yates, D., Chen, F., et al. (2011). High-resolution coupled climate runoff simulations of seasonal snowfall over Colorado: A process study of current and warmer climate. *Journal of Climate*, *24*(12), 3015–3048. https://doi.org/10.1175/2010JCLI3985.1

Rasmussen, R. M., Chen, F., Liu, C., Ikeda, K., Prein, A., Kim, J., et al. (2023). Conus404: The NCAR–USGS 4-km long-term regional hydroclimate reanalysis over the conus. *Bulletin of the American Meteorological Society*, *104*(8), E1382–E1408. https://doi.org/10.1175/BAMS-D-21-0326.1

Rasmussen, R. M., Liu, C., Ikeda, K., & Dominguez, F. (2022). Multi-decadal convection-permitting simulation of current climate over South America using WRF [Dataset]. *NSF National Center for Atmospheric Research*. https://doi.org/10.5065/6XQW-ZB02

Ruiz-Vásquez, M., Arias, P. A., Martínez, J. A., & Espinoza, J. C. (2020). Effects of Amazon basin deforestation on regional atmospheric circulation and water vapor transport towards tropical South America. *Climate Dynamics*, *54*, 4169–4189. https://doi.org/10.1007/S00382-020-05223-4/FIGURES/12

Sodemann, H., Wernli, H., & Schwierz, C. (2009). Sources of water vapour contributing to the Elbe flood in August 2002—A tagging study in a mesoscale model. *Quarterly Journal of the Royal Meteorological Society*, *135*(638), 205–223. https://doi.org/10.1002/QJ.374

Sorí, R., Stojanovic, M., Nieto, R., Liberato, M. L. R., & Gimeno, L. (2022). Spatiotemporal variability of droughts in the Congo River basin. In *Congo basin hydrology, climate, and biogeochemistry* (pp. 187–203). American Geophysical Union (AGU). https://doi.org/10.1002/9781119657002.ch11

Staal, A., Flores, B. M., Aguiar, A. P. D., Bosmans, J. H., Fetzer, I., & Tuinenburg, O. A. (2020). Feedback between drought and deforestation in the Amazon. *Environmental Research Letters*, *15*(4), 044024. https://doi.org/10.1088/1748-9326/AB738E

Stratton, R. A., Senior, C. A., Vosper, S. B., Folwell, S. S., Boutle, I. A., Earnshaw, P. D., et al. (2018). A Pan-African convection-permitting regional climate simulation with the met office unified model: CP4-Africa. *Journal of Climate*, *31*(9), 3485–3508. https://doi.org/10.1175/JCLI-D-17-0503.1

Tuinenburg, O. A., Theeuwen, J. J., & Staal, A. (2020). High-resolution global atmospheric moisture connections from evaporation to precipitation. *Earth System Science Data*, *12*(4), 3177–3188. https://doi.org/10.5194/ESSD-12-3177-2020

van der Ent, R. J., & Tuinenburg, O. A. (2017). The residence time of water in the atmosphere revisited. *Hydrology and Earth System Sciences*, *21*(2), 779–790. https://doi.org/10.5194/hess-21-779-2017

Wallace, B., & Minder, J. R. (2024). The North American monsoon precipitation response to climate warming at convection-permitting scales. *Climate Dynamics*, *62*(1), 497–524. https://doi.org/10.1007/s00382-023-06920-6

Wang, X., Zhang, Z., Zhang, B., Tian, L., Tian, J., Arnault, J., et al. (2023). Quantifying the impact of land use and land cover change on moisture recycling with convection-permitting WRF-tagging modeling in the agro-pastoral ecotone of northern China. *Journal of Geophysical Research: Atmospheres*, *128*(8), e2022JD038421. https://doi.org/10.1029/2022jd038421

Worden, S., Fu, R., Chakraborty, S., Liu, J., & Worden, J. (2021). Where does moisture come from over the Congo Basin? *Journal of Geophysical Research: Biogeosciences*, *126*(8), e2020JG006024. https://doi.org/10.1029/2020JG006024

Yang, Z., & Dominguez, F. (2019). Investigating land surface effects on the moisture transport over South America with a moisture tagging model. *Journal of Climate*, *32*(19), 6627–6644. https://doi.org/10.1175/JCLI-D-18-0700.1

Yang, Z., Qian, Y., Liu, Y., Berg, L. K., Hu, H., Dominguez, F., et al. (2019). Irrigation impact on water and energy cycle during dry years over the United States using convection-permitting WRF and a dynamical recycling model. *Journal of Geophysical Research: Atmospheres*, *124*(21), 11220–11241. https://doi.org/10.1029/2019JD030524

Zemp, D. C., Schleussner, C. F., Barbosa, H. M., Hirota, M., Montade, V., Sampaio, G., et al. (2017). Self-amplified Amazon forest loss due to vegetation-atmosphere feedbacks. *Nature Communications 2017*, *8*(1), 1–10. https://doi.org/10.1038/ncomms14681

Zou, L., Zhou, T., & Zhao, Y. (2024). How does regional convection-permitting modeling improve the simulation of the atmospheric water cycle in spring over the Tibetan Plateau? *Journal of Geophysical Research: Atmospheres*, *129*(15), e2024JD040964. https://doi.org/10.1029/2024JD040964

## References From the Supporting Information

Hersbach, H., Bell, B., Berrisford, P., Hirahara, S., Horányi, A., Muñoz-Sabater, J., et al. (2020). The ERA5 global reanalysis. *Quarterly journal of the royal meteorological society*, *146*(730), 1999–2049. https://doi.org/10.1002/qj.3803

Hong, S.-Y., & Lim, J.-O. J. (2006). The WRF single-moment 6-class microphysics scheme (WSM6). *Asia-Pacific Journal of Atmospheric Sciences*, *42*(2), 129–151.

Hong, S.-Y., Noh, Y., & Dudhia, J. (2006). A new vertical diffusion package with an explicit treatment of entrainment processes. *Monthly Weather Review*, *134*(9), 2318–2341. https://doi.org/10.1175/mwr3199.1

Huffman, G. J., Bolvin, D. T., Braithwaite, D., Hsu, K.-L., Joyce, R. J., Kidd, C., et al. (2020). Integrated multi-satellite retrievals for the global precipitation measurement (Gpm) mission (Imerg). In V. Levizzani, C. Kidd, D. B. Kirschbaum, C. D. Kummerow, K. Nakamura, & F. J. Turk (Eds.), *Satellite precipitation measurement: Volume 1* (pp. 343–353). Springer International Publishing. https://doi.org/10.1007/978-3-030-24568-9_19

Huffman, G. J., Bolvin, D. T., Joyce, R., Kelley, O. A., Nelkin, E. J., Portier, A., et al. (2023). *Imerg v07 release notes*. Goddard Space Flight Center: Greenbelt.

Iacono, M. J., Delamere, J. S., Mlawer, E. J., Shephard, M. W., Clough, S. A., & Collins, W. D. (2008). Radiative forcing by long-lived greenhouse gases: Calculations with the Aer radiative transfer models. *Journal of Geophysical Research*, *113*(D13). https://doi.org/10.1029/2008jd009944

Kain, J. S. (2004). The Kain–Fritsch convective parameterization: An update. *Journal of Applied Meteorology*, *43*(1), 170–181. https://doi.org/10.1175/1520-0450(2004)043<0170:tkcpau>2.0.co;2

Martens, B., Miralles, D. G., Lievens, H., van der Schalie, R., de Jeu, R. A. M., Fernández-Prieto, D., et al. (2017). Gleam v3: Satellite-based land evaporation and root-zone soil moisture. *Geoscientific Model Development*, *10*(5), 1903–1925. https://doi.org/10.5194/gmd-10-1903-2017

Niu, G.-Y., Yang, Z.-L., Mitchell, K. E., Chen, F., Ek, M. B., Barlage, M., et al. (2011). The community NOAH land surface model with multiparameterization options (Noah-MP): 1. Model description and evaluation with local-scale measurements. *Journal of Geophysical Research*, *116*(D12), D12109. https://doi.org/10.1029/2010jd015139

Zhang, C., & Wang, Y. (2017). Projected future changes of tropical cyclone activity over the western north and south Pacific in a 20-km-mesh regional climate model. *Journal of Climate*, *30*(15), 5923–5941. https://doi.org/10.1175/JCLI-D-16-0597.1